Chloroplast redox status modulates the cell expansion phase of leaf development associated to changes in proteasome activity and endoreduplication index

Martín L. Mayta[1† ‡], Rocío C. Arce[1‡], Michael Melzer[2], Mohammad-Reza Hajirezaei[2], Anabella F. Lodeyro[1]*, Néstor Carrillo[1]*

[1]*Instituto de Biología Molecular y Celular de Rosario (IBR-UNR/CONICET), Facultad de Ciencias Bioquímicas y Farmacéuticas, Universidad Nacional de Rosario (UNR), 2000 Rosario, Argentina.*

[2]*Leibniz Institute of Plant Genetics and Crop Plant Research, OT Gatersleben, Corrensstrasse, D-06466 Stadt Seeland, Germany.*

[†]*Present address: Centro para la Investigación en Ciencias de la Salud, Facultad de Ciencias de la Salud, Universidad Adventista del Plata, 25 de Mayo 99, E3103XAF, Libertador San Martín, Entre Ríos, Argentina.*

[‡]These authors contributed equally to the work.

*Correspondence to: Anabella Lodeyro, lodeyro@ibr-conicet.gov.ar; Néstor Carrillo, carrillo@ibr-conicet.gov.ar.

Summary

Leaf growth is sustained by successive phases of cell proliferation and expansion that determine the final organ size. The rate and extension of these phases are modulated by several developmental and environmental cues. We show herein that changes in the redox status of tobacco chloroplasts caused by introduction of the alternative electron shuttle flavodoxin led to decreased leaf size. Flavodoxin activity as electron sink prevented over-reduction of the photosynthetic electron transport chain and propagation of reactive oxygen species. These effects correlated with significantly lower rates of cell expansion in leaves of flavodoxin-expressing plants. Neither the duration of the expansion phase nor the rate and extension of the proliferative stage were affected by the presence of the alternative electron carrier, resulting in smaller leaf cells without significant differences in their numbers. Cells from transformed plants contained fewer chloroplasts of wild-type size, but their cellular coverage was increased due to cell size reduction. Chloroplast redox modulation of leaf development was associated to increased proteasomal activity and lower endoreduplication. The results identify a new player in the global regulation of plant organ growth, as represented by plastid-generated redox signals, and underscore the value of alternative electron shuttles to investigate the signaling role of chloroplast oxido-reductive biochemistry in plant developmental pathways.

Keywords: leaf development, flavodoxin, photosynthesis, chloroplast redox status, proteasome, endoreduplication.

Significance Statement

Chloroplasts play a central role during plant growth through the generation and transmission of redox-based signals. Here we show that changes in chloroplast redox status due to expression of the alternative electron sink flavodoxin affected the rates of cell expansion during leaf development, resulting in significant leaf size reduction. Flavodoxin effects were associated to increased proteasome activity and lower endoreduplication. Our results identify a new player in the global regulation of leaf growth.

Introduction

Oxygenic photosynthesis contributes most of the global enthalpy of living systems and determines the composition of the atmosphere (Nelson, 2013). At a planetary scale, about 50% of this all-important process takes place in leaves, which are therefore at the core of plant growth, seed production and ultimately, agriculture. Leaf size, in particular, defines the maximal photosynthetic area and is a key factor for plant performance within a given species (Ren *et al.*, 2019). After initiation as lateral outgrowths from shoot apical meristems, foliar development proceeds through two stages: an initial phase characterized by successive cell divisions, in which specific structures such as trichomes and stomata begin to form, followed by post-mitotic cell expansion with the transition front progressing in a basipetal direction from the leaf tip (Donnelly *et al.*, 1999; Traas and Monéger, 2010; Gonzalez *et al.*, 2010; 2012). Since dividing cells also expand, the term proliferation is preferred to describe the first phase (Gonzalez *et al.*, 2010; Andriankaja *et al.*, 2012; Kalve *et al.*, 2014)

Given its importance for plant growth and crop yield, foliar development has been extensively studied, revealing a complex and plastic process whose outcome in terms of size and shape depends on genetic background, leaf position and environmental conditions (Andriankaja *et al.*, 2012). Despite the richness of information gathered, determination of leaf size remains intriguing in various aspects. On the one hand, leaf cell proliferation and expansion are controlled by the interplay of a network of endogenous factors such as phytohormones, reactive oxygen species (ROS), sugars and other signals which in turn affect the expression of a multitude of genes (Traas and Monéger, 2010; Bar and Ori, 2014). In a fixed environment, final leaf size and shape are so uniform for a given species that these morphological features have been extensively used for taxonomic classification, but at the same time they can change dramatically by mutation of a single gene (Barkoulas *et al.*, 2008; Kalve *et al.*, 2014).

Chloroplasts play a central role during plant growth, not only by providing energy and nutrients via photosynthesis but also through the generation and transmission of redox-based signals (Muñoz and Munné-Bosch, 2018). While the contribution of chloroplast oxido-reductive processes (including ROS

propagation) in modulating cell death and environmental stress tolerance is well supported (Petrov *et al.*, 2015; Schmidt *et al.*, 2016; Rossi *et al.*, 2017; Su *et al.*, 2018; Gómez *et al.*, 2019), their involvement in early leaf development has only recently been recognized. For instance, timely exit from the proliferative phase has been shown to require complete chloroplast biogenesis and can be prevented by herbicides acting on the photosynthetic machinery (Andriankaja *et al.*, 2012). Moreover, several mutants lacking chloroplast proteins differentially expressed during leaf development display severe growth phenotypes including major reductions in organ size (van Dingenen, Blomme, *et al.*, 2016; van Dingenen, de Milde, *et al.*, 2016). The nature of the signals exiting chloroplasts remains yet to be determined, but they could be linked to oxido-reductive pathways of the organelle, in particular to the redox status of the photosynthetic electron transport chain (PETC) and/or plastid-generated ROS. In this sense, the intervention of the PETC with alternative electron shuttles from plants or cyanobacteria might be a tool to understand (and manipulate) the retrograde signals transmitted by the chloroplasts that influence leaf development (Dietz *et al.*, 2016).

Cyanobacterial flavodoxin (Fld) provides a remarkable example of this approach. Fld is a low-potential FMN-containing electron carrier which mediates essentially the same reactions as the iron-sulfur protein ferredoxin (Fd), including electron shuttling from photosystem (PS) I at the PETC to a plethora of metabolic, dissipative and regulatory processes (Lodeyro *et al.*, 2012; Pierella Karlusich *et al.*, 2014). In cyanobacteria and oceanic algae, Fld expression is induced by most environmental stresses to take over the activities of Fd, whose levels are down-regulated under such conditions allowing growth and reproduction of the microorganism in the adverse environment (Pierella Karlusich *et al.*, 2014). Fld-encoding genes are absent from plant genomes (Pierella Karlusich *et al.*, 2015), but the introduction of a plastid-targeted Fld in transgenic lines resulted in increased tolerance to multiple sources of biotic and abiotic stress, relieving the excess of excitation energy on the PETC and mitigating photo-oxidative damage and ROS propagation (Tognetti *et al.*, 2006, 2007; Zurbriggen *et al.*, 2008, 2009; Coba de la Peña *et al.*, 2010; Li *et al.*, 2017; Rossi *et al.*, 2017).

While the improved stress tolerance of plants expressing Fld in chloroplasts could be associated with the functional replacement of declining Fd (Blanco *et al.*, 2011), the presence of this additional redox player elicited phenotypic effects even in transgenic plants grown under normal conditions, in which Fd and Fld accumulated to similar levels (Tognetti *et al.*, 2006; Ceccoli *et al.*, 2012). They included higher pigment contents and photosynthetic activity per leaf cross-section (Tognetti *et al.*, 2006; Ceccoli *et al.*, 2012; Rossi *et al.*, 2017), and delayed leaf senescence (Mayta *et al.*, 2018). In terms of the chloroplast redox status, Fld activity prevented ROS build-up during stress (Tognetti *et al.*, 2006; Zurbriggen *et al.*, 2009) and senescence (Mayta *et al.*, 2018), and increased plastoquinone oxidation state under normal growth conditions (Gómez *et al.*, 2020). Moreover, about 1,000-1,500 leaf transcripts changed their expression patterns in response to Fld presence in tobacco and potato, respectively (Pierella Karlusich *et al.*, 2017, 2020).

Fld thus provides a tool to alter the chloroplast redox balance in a customized way and to investigate the consequences of this intervention on plant physiology and development. Indeed, Fld expression led to decreased plant and leaf size in several species (Li *et al.*, 2017; Su *et al.*, 2018; Mayta et al., 2019), prompting for a more detailed evaluation of these effects. We describe herein the impact of Fld presence on leaf development by employing tobacco plants expressing the flavoprotein in chloroplasts. When grown under controlled conditions, leaves from *pfld* plants were significantly smaller than wild-type (WT) counterparts as a consequence of slower leaf cell expansion without changes in cell proliferation or the timing of the different transitions. Fld presence also affected chloroplast number and pigment contents. ROS accumulation during early developmental stages of WT plants was attenuated in the transformants. The effect of Fld on organ size was associated to increased proteasomal activity and correlated with a lower degree of endoreduplication. The possible contribution of chloroplast redox signals to the onset and progression of leaf development is discussed in the light of these results.

Results

Fld expression in chloroplasts of tobacco plants decreases the rate of leaf cell expansion

WT and Fld-expressing plants were grown under controlled chamber conditions (Experimental procedures) to isolate the effects of the flavoprotein on leaf development from those on stress protection that might also affect organ size. Independent tobacco lines *pfld*5-8 and *pfld*4-2 contain similar levels of Fld in chloroplasts and display the same phenotype with respect to stress tolerance (Tognetti *et al.*, 2006). The first true leaf emerging after the cotyledons was numbered 1 and used as a model of foliar growth. Typical phenotypes of WT and *pfld* plants at 35 days post-germination (dpg) showed that Fld expression in plastids led to a significant decrease in leaf size in the absence of environmental pressures (Figure 1a-c). Size reduction could be visualized from 12 dpg and affected all leaves (Figure S1a, b). A homozygous line expressing high levels of Fld in the cytosol (*cfld*1-4; Tognetti *et al.*, 2006) displayed a WT phenotype (Figure 1a-c; Figure S1a, b), indicating that chloroplast location was mandatory for the Fld effects. These results thus concur with the size reduction reported for creeping bentgrass, Arabidopsis and tomato plants expressing a plastid-located Fld (Li *et al.*, 2017; Su *et al.*, 2018; Mayta *et al.*, 2019).

As a first step to characterize the mechanism underlying this effect, different regions of leaf 1 were sampled (Figure 1d) to estimate cell size and numbers by microscopic analysis. At 35 dpg, the average area of mesophyll cells belonging to the palisade parenchyma was decreased by ~50% in mature *pfld* leaves compared to WT and *cfld* siblings (Figure 1e, f), correlating with the reduction in leaf area (Figure 1c). Total cell numbers, instead, were not significantly modified (Figure 1g). Epidermal pavement cells exhibited a similar pattern (Figure S2a-c), whereas stomatal index was not affected by the presence of the flavoprotein (Figure S2d). When the same type of experiment was carried out at 6 dpg, no significant differences in cell size were observed between lines (Figure S3). The results suggest that Fld-dependent changes in chloroplast redox status did not affect the early stages of leaf development usually associated to cell proliferation, but had a detrimental impact on cellular expansion.

To determine if the smaller cells of *pfld* leaves were the result of lower rates of cell expansion and/or a shortening of the expansion phase, a kinematic analysis

of leaf and cell development was carried out in WT and *pfld* plants. As shown in Figure 2a, average areas of leaf 1 were similar for all lines up to 9 dpg, but *pfld* leaves grew significantly slower than WT counterparts after that time. Growth ceased at about 20 dpg in all lines (Figure 2a), indicating that the onset of leaf maturity was not affected by the presence of the additional redox carrier. Leaves emerging later than leaf 1 displayed similar behavior, as illustrated for leaf 10 in Figure S4.

Cellular analysis over time showed a good correlation with these phenotypic features. Post-mitotic expansion continued up to ~20 dpg, although *pfld* cells expanded at lower rates compared to WT siblings (Figure 2b). Cell numbers increased at similar rates in WT and *pfld* leaves, reaching their maxima at ~12 dpg in all cases (Figure 2c). The effect of the flavoprotein was also reflected in the number of cells per leaf cross-section, which is the basis on which pigment levels and photosynthetic activities are usually reported. This number declined steadily throughout organ development, but *pfld* leaves began to pack a higher number of smaller cells per area upon entering the expansion phase, stabilizing at a ~2-fold higher cell density than WT siblings at the end of this stage (Figure S5). The results thus show that Fld activity specifically affected expansion rates with no appreciable effects on cell proliferation or the timing of exit from proliferation and expansion (Figure 2b, c).

Fld presence affects chloroplast number and chlorophyll contents

Previous observations have shown that *pfld* plants contained more *Chl* and carotenoids per leaf area than WT siblings, which correlated with increased photosynthetic activity (Tognetti *et al.*, 2006; Rossi *et al.*, 2017; Gómez *et al.*, 2020). Analysis of pigment contents along the various stages of leaf development confirmed those observations (Figure S6). Differences between lines were marginal at the proliferative stage, but the levels of *Chl a* and carotenoids increased in *pfld* leaves well above those of their WT counterparts from the beginning of the expansion phase (Figure S6a, d), whereas *Chl b* contents only began to diverge between lines at the onset of leaf maturity (Figure S6b). Noteworthy, *Chl a* continued to accumulate in *pfld* leaves up to 25 dpg, when WT levels had already started to decline (Figure 6a). A delay in leaf

senescence, including protracted pigment degradation, has been already reported for *pfld* plants (Mayta et al., 2018) and might explain this behavior.

Then, Fld activity affected both cell density and pigment contents per area (Supplementary Figures S5, S6). During expansion and early leaf maturity the increase in cell packing surpassed pigment build-up, and *pfld* cells actually contained less *Chl* and carotenoid than WT siblings (Figure S7). The two Fld effects eventually cancelled each other at 25-30 dpg, and mature leaves from all lines exhibited similar pigment contents per individual cell (Figure S7). Individual chloroplasts isolated from mature leaves of *pfld* plants contained 30-40% more *Chl* than WT counterparts (Figure 3a), indicating that the number of chloroplasts per cell is significantly lower in the transformants (Figure 3b). This decrease likely reflects spatial constraints on plastid proliferation in the smaller cells of *pfld* leaves. Indeed, the positive correlation between plastid proliferation and cell size has been reported previously (Kawade *et al.*, 2013).

We then investigated if these cellular features were accompanied by changes in plastid size and/or structure. Chloroplasts were visualized by transmission electron microscopy of palisade parenchyma cells throughout leaf development (Figure S8a). Image analysis of the resulting micrographs using ImageJ (Experimental procedures) failed to show consistent differences between lines in chloroplast ultrastructure, average area or grana stacking, as illustrated for WT and the *pfld*5-8 line in Figure S8a-c. Despite their lower number and similar size, chloroplast coverage per cell was higher in mature *pfld* leaves (Figure 3c), as the reduction in cell size offset the decline in plastid numbers. The collected results indicate that the increased levels of photosynthetic pigments per area in *pfld* leaves (Tognetti *et al.*, 2006; Ceccoli *et al.*, 2012; Gómez *et al.*, 2020) stem from the combination of two factors: a higher density of smaller cells per unit of leaf cross-section (Figure S3) and increased pigment contents per chloroplast at leaf maturity (Figure 3a).

ROS build-up was prevented by Fld expression in developing tobacco leaves

Immature leaves have been reported to display lower photosynthetic activities compared to fully expanded counterparts, a feature associated to an incomplete assembly of the PETC during the early stages of leaf development (Juvany *et al.*, 2013; Huang *et al.*, 2018). Indeed, genes involved in *Chl* biosynthesis are induced earlier than those encoding photosynthetic enzymes (Andriankaja *et al.*, 2012). We therefore hypothesized that light capture with diminished capacity to perform photochemistry could lead to over-reduction of the partially assembled PETC and augmented electron leakage to oxygen. Redox-based signals (including ROS) generated during this process might act as developmental cues affecting early leaf growth, and relief of the excess excitation energy by additional electron sinks such as Fld could be related to the leaf phenotype of *pfld* plants.

Rates of electron transport through the PETC were thus measured at various times of leaf development. Small size, especially at the early stages, precluded the use of leaf 1 for photosynthetic determinations, so leaf 10 was used instead to estimate the quantum yields of PSI and PSII (ϕ_{PSI} and ϕ_{PSII}, respectively), which provide a measure of electron flow through these photosystems. Measurements carried out in WT plants at 44 dpg, when cells of leaf 10 are expected to be for the most part at the proliferative stage, yielded significantly lower ϕ_{PSI} and ϕ_{PSII} values than those of fully expanded mature leaves (Figure 4a, b), in agreement with previous reports (Juvany *et al.*, 2013; Huang *et al.*, 2018). Quantum yields increased steadily with leaf age for both photosystems, reaching a maximum at the end of the expansion phase and then declining to initial values (Figure 4a, b). ROS levels were determined in cleared extracts of the same WT leaves. They showed a negative correlation with electron transport rates, being maximal during proliferation and at late maturity (Figure 4c). The results suggest that at least part of the electron flow estimated by ϕ_{PSI} and ϕ_{PSII} was used to reduce oxygen to ROS.

Chloroplast Fld did not improve photosynthetic activity during proliferation and early expansion of *pfld*5-8 leaves. The decline of electron transport rates in older leaves was instead partially prevented by the plastid-targeted flavoprotein (Figure 4a, b), in line with previous observations (Mayta *et al.*, 2018). Despite the lack of Fld influence on the photosynthetic activity of immature leaves, the

flavoprotein electron shuttle decreased ROS propagation during all stages of leaf development (Figure 4c).

Fld effects on leaf size correlated with increased activity of the 26S proteasome

Among the various factors influencing organ size, loss of function of the 26S proteasome has been shown to result in leaf enlargement via increased cell expansion (Kurepa *et al.*, 2009; Sonoda *et al.*, 2009), whereas its up-regulation by over-expressing an upstream regulator had the opposite effect (Nguyen *et al.*, 2013). Noteworthy, Fld presence in chloroplasts led to generalized induction of proteasomal subunits in leaves of tobacco and potato plants cultured under normal growth conditions, as revealed by microarray analysis (Pierella Karlusich *et al.*, 2017; 2020). This observation was confirmed and extended for selected components of both the 20S proteasomal core and the 19S regulatory subunit (Figure 5a) by real-time reverse-transcription quantitative PCR (qRT-PCR). *RPN9*, *a6-SU* and *UMP1* were previously validated as up-regulated proteasome genes in *pfld*5-8 plants (Pierella Karlusich *et al.*, 2017), while *RPT2a* and *RPT5a* were chosen because of their involvement in leaf size regulation through modification of cell expansion (Cho *et al.*, 2006; Sonoda *et al.*, 2009; Sako and Yamaguchi, 2010). Irrespective of the expression pattern of the gene assayed, transcript levels were higher in *pfld*5-8 leaves at virtually all developmental stages except proliferation for *RPN9* and *RPT5a* (Figure 5b-f).

Induction of individual proteasomal subunits correlated with increased proteasome activity in *pfld*5-8 leaves compared to WT counterparts, but only during the cell expansion phase (Figure 5g). Activities did not show significant differences between lines in mature leaves and interestingly, were lower in *pfld* plants compared to WT siblings during proliferation (Figure 5g). Involvement of proteasome activity in Fld-dependent modulation of leaf size was further supported by the observation that Fld effects were partially suppressed upon exposure of the plants to sub-lethal concentrations of the proteasome inhibitor MG132 (Figure 5h, i).

Decreased cell size in *pfld* leaves was associated with lower endoreduplication

Endoreduplication is a modified version of the cell cycle that lacks the M phase and has been associated to increased cell and organ size (Tsukaya, 2008). Although further research has shown that this correlation is not universal (Tsukaya, 2019, and references therein), various authors reported that enlarged cells in an *RPT2a* and *RPT5a* mutants, deficient in proteasomal activity, showed extended endoreduplication at the early stages of development (Sonoda *et al.*, 2009; Sako and Yamaguchi, 2010). We therefore investigated the ploidy level in leaf 1 of WT and *pfld* plants using flow cytometry. At 25 dpg, most WT DNA was in the 4C form, whereas the majority of *pfld* cells were diploid with lower contribution of 4C (Figure 6a, b). Accordingly, the endoreduplication index was significantly higher in the wild type (Figure 6c), correlating with increased cell size.

Discussion

Leaf development relies on the coordination of cell proliferation and expansion. The first of these processes sets the total number of cells in a leaf, whereas post-mitotic cell expansion determines the final cell size, so that both processes contribute to determine overall organ size (Gonzalez *et al.*, 2012; Kalve *et al.*, 2014). The transition from proliferation into expansion proceeds basipetally and occurs quite abruptly during leaf development (Kazama *et al.*, 2010; Andriankaja *et al.*, 2012). Results obtained through the use of mutants and inhibitors of chloroplast biogenesis indicate that the onset of cell expansion depends on the establishment of a functional photosynthetic machinery and its associated retrograde signaling (Andriankaja *et al.*, 2012; Hudik *et al.*, 2014; van Dingenen, Blomme, *et al.*, 2016). On the other hand, redox-based signals, including ROS generated during photooxidative stress, have been shown to modulate leaf development (Dietz et al., 2016), and chloroplasts, with their rich oxido-reductive metabolism, should make a significant contribution to this process (Juvany *et al.*, 2013; Muñoz and Munné-Bosch, 2018). We show here that introduction of the alternative electron sink Fld, which is known to effectively relieve the excitation pressure on the PETC (Gómez *et al.*, 2020),

resulted in decreased leaf size in tobacco plants (Figure 1; Figure S1). When present in chloroplasts, Fld might be interfering with retrograde redox signaling involved in leaf development. Photooxidative stress is expected to occur in young leaves when the photosynthetic machinery is still under construction and the energy dissipation mechanisms are not yet fully operational. These limitations could lead to over-reduction of the PETC and increased ROS propagation in immature plastids (Szymańska and Kruk, 2008; Lepeduš *et al.*, 2011; Juvany *et al.*, 2013; Muñoz and Munné-Bosch, 2018). A model summarizing these observations is given in Figure 7a. By accepting reducing equivalents from PSI, Fld limits ROS accumulation (Figure 4c) and increases the oxidation state of key signaling components of the PETC such as plastoquinone (Gómez *et al.*, 2020). It is worth noting, within this context, that Fld does not simply act as a dissipative electron sink device such as the Mehler-Asada cycle or chlororespiration, but instead it delivers the surplus of reducing equivalents to productive redox pathways of the chloroplast. In doing so, Fld protects photosynthesis and limits ROS build-up through the various stages of leaf development (Figure 7a).

Since leaf size can be modified by the addition of sugars, the role of photosynthesis has been usually associated to the supply of carbohydrates, not only as a source of nutrients and energy but also as signals (Smeekens and Hellmann, 2014; van Dingenen, de Milde, *et al.*, 2016), raising the possibility that the Fld effect could be mediated by increased carbon metabolism resulting from incorporation of the additional electron carrier into the photosynthetic process. Metabolic profiling of *pfld* leaves from plants grown under normal conditions suggest otherwise: steady-state levels of soluble carbohydrates such as sucrose, glucose and fructose were not affected by the activity of the flavoprotein in chloroplasts (Tognetti *et al*., 2007: Mayta *et al*., 2018). Moreover, Fld and sugars influence organ development in different ways. Sucrose, for instance, increases final leaf size by promoting cell proliferation and postponing exit from this phase (van Dingenen, de Milde, *et al.*, 2016), whereas Fld specifically alters the rates of cell expansion, without affecting the timespan of the phases (Figure 2; Figure S4). Also, plant exposure to sugars resulted in smaller chloroplasts in mesophyll cells (van Dingenen, de Milde, *et al.*, 2016).

Fld expression, instead, had no significant effect on plastid size or ultrastructure (Figure S8). Although further research is necessary to properly settle this issue, the results suggest that Fld impact on leaf development was not associated to sugar signaling.

As a first step to unravel the mechanisms by which chloroplast redox signals might control leaf cell expansion it is necessary to identify their cellular targets. Transcriptional profiling of *pfld* plants grown under normal conditions revealed that levels of over 1,000 leaf transcripts were differentially affected by the presence of the flavoprotein, with generalized induction of proteasomal subunits being the most remarkable feature of the plant response to Fld presence (Pierella Karlusich *et al.*, 2017; 2020). This up-regulation correlated with an increase in proteasome activity, which initiated upon transition into the expansion phase of leaf development (Figure 5), namely, the same developmental stage at which chloroplast Fld exerted its differential effect on leaf growth (Figure 2a; Figure S4). Several lines of evidence support the central role played by protein degradation via the proteasome in the determination of organ size. Pharmacological approaches and analysis of loss-of-function mutants indicate that higher proteasome activity decreases leaf size, and *vice versa* (Kurepa and Smalle, 2008; Sonoda *et al.*, 2009; Nguyen *et al.*, 2013). Interestingly, different components of the 26S complex were shown to operate at various levels of the organ development pathway. For instance, plants deficient in the ubiquitin receptor DA1 or the E3 ligase BIG BROTHER exhibit leaf enlargement caused by changes in the rate and duration of the proliferative phase (Disch *et al.*, 2006; Vanhaeren *et al.*, 2017), whereas inactivation of the AAA ATPase RPT2a, belonging to the 19S regulatory subunit, led to a similar outcome by increased cell expansion (Kurepa *et al.*, 2009; Sonoda *et al.*, 2009).

While over-expression of individual proteasomal subunits do not usually affect its total activity or leaf size (Kurepa and Smalle, 2008), Fld presence led to generalized induction of proteasomal components and resulted in a concomitant increase in activity (Figure 5a-g). A similar global induction has been accomplished through constitutive expression of the upstream positive regulator RPX (Nguyen *et al.*, 2013). Involvement of proteasome function in the phenotypes elicited by Fld and RPX was confirmed by partial reversion of the

leaf size decrease using specific inhibitors of proteasome activity (Figure 5h, i; Nguyen *et al.*, 2013). Leaf growth reduction in *pfld* tobacco plants was accompanied by a decline in DNA polyteny (Figure 6), a correlation already reported for Arabidopsis *RPT2a* and *RPT5a* mutants (Sonoda *et al.*, 2009; Sako and Yamaguchi, 2010). We propose that down-regulation of this process occurs downstream of the proteasome (Figure 7b). Indeed, RPT2a has been shown to negatively regulate endoreduplication in Arabidopsis trichomes and epidermal cells (Sako *et al.*, 2010), in line with the observations reported here.

As a working hypothesis, we thus propose that redox-based signals transmitted by the chloroplast affect proteasomal expression and activity, which in turn modulate cellular processes involved in organ size determination, including endoreduplication (Figure 7b). Redox regulation of the proteasome has been normally associated with oxidative rather than reductive stimuli (Lefaki *et al.*, 2017), although NADH was shown to stabilize the 26S complex in animal cells (Tsvetkov *et al.*, 2014). Redox signals generated in chloroplasts can be both oxidative (i.e., ROS) or reductive (namely, over-reduction of the PETC), and Fld could mitigate both of them. Further research will be required to distinguish which of these possible signals is affecting proteasome expression and function during leaf development. For instance, a combination of alternative electron sinks accepting electrons from different components of the PETC might help to dissect the nature of the redox signaling relay.

In conclusion, we report here that customized alterations of chloroplast redox status by the introduction of an alternative electron transfer pathway have a direct impact on final leaf size (Figure 7). Research on chloroplast retrograde regulation has gained momentum in recent years, leading to the identification of various plastid-generated signals able to affect nuclear gene expression. They include intermediates of carotenoid and tetrapyrrole biosynthesis, phytohormones, ROS-related processes, the redox poise of the PETC and changes in metabolite pools, most remarkably sugars (Pfalz *et al.*, 2012; Tanaka and Hanaoka, 2013; Dietz *et al.*, 2016; Hernández-Verdeja and Strand, 2018; Shimizu *et al.*, 2019; Loudya *et al.*, 2020). Also, redox inputs affecting leaf size can be generated in cellular compartments different from plastids (Lu *et al.*, 2014; Considine *et al.*, 2017). These developmental cues likely interact in a

cooperative way to tailor organ development. Understanding how this multiplicity of pathways coordinate and cross-talk in the determination of leaf size and shape constitutes a most exciting goal of plant biology with potential impact in agriculture.

Experimental procedures

Plant material and growth conditions

Wild-type, *pfld* and *cfld* tobacco plants (*Nicotiana tabacum* cv. Petit Havana) were grown autotrophically in soil at 250 µmol photons m^{-2} s^{-1} with a 16-h photoperiod, 28°C/20°C and a relative humidity of 60-80% (chamber conditions). The first true leaf emerging after the cotyledons was termed 1. The design and preparation of homozygous *pfld* and *cfld* plants have been described elsewhere (Tognetti *et al.*, 2006).

Kinematic leaf growth analysis

For leaf 1 area measurements, individual leaves (8-12 per genotype) were harvested at different dpg and immediately fixed in 96% (v/v) ethanol until complete pigment removal (~12 h). Clearing was completed by incubation in 85% (w/v) lactic acid for 1 week. Leaves were mounted in lactic acid on glass slides, photographed at low magnification (0.75×) under a dissecting microscope (Leica MZFLIII, Germany) and their areas measured with the ImageJ software (Rasband, 1997–2008, http://rsb.info.nih.gov/ij/). For leaf 10 (tenth true leaf counting from the bottom) growth analysis, 12-14 plants of each genotype were grown in 3-L pots until leaf 10 became visible in the shoot apical meristem (~44 dpg). Leaf contour was manually drawn in a paper sheet at different dpg during development. Foliar area was obtained from the drawn leaf contour using ImageJ.

Leaf *Chl* contents were determined spectrophotometrically after extraction with 96% (v/v) ethanol (Lichtenthaler, 1987).

Structural analysis of leaf tissue by light and transmission electron microscopy

To determine cell size and number, the first true leaves of at least 8 independent plants per genotype were harvested at different dpg and cleared in 96% (v/v) ethanol as indicated above. Cell images were acquired through differential interference contrast (DIC) microscopy (Olympus BH2, Tokyo, Japan), and areas quantified with ImageJ. Leaf cells from the adaxial sub-epidermal palisade parenchyma layer or the adaxial epidermis were observed by DIC microscopy. Cell areas were determined, and leaf blade area was divided by the average cell area to calculate the total number of cells. At least 100 cells were measured in 4 different regions to calculate mean cell areas (Figure 1d). The stomatal index (SI) was calculated using the formula: SI = [number of stomata/ (number of other epidermal cells + number of stomata)] × 100, and averaged from 4 independent DIC images of the adaxial epidermis per plant.

For chloroplast ultrastructure, 2-mm^2 cuttings from the central part of leaf 1 from 4 different plants of WT and *pfld* lines at different dpg were used as samples for histological and ultrastructural examination. Conventional and microwave-assisted fixation substitution, resin embedding, sectioning, and microscopic analyses were performed as described (Kraner *et al.*, 2017). Chloroplast coverage was defined as the percentage of chloroplast area per cell area, and calculated with ImageJ in palisade parenchyma cells using TEM images of chloroplasts (10.000 or 13.000×) of transverse sections from fully expanded leaf 1 tissue at 25 dpg.

Determination of photosynthetic parameters

C*hl a* fluorescence and P700 absorption were simultaneously measured on leaf 10 at 25°C using a Dual-PAM-100 system (Heinz Walz, Effeltrich, Germany). In all cases, leaves were dark-adapted for 3 h to inactivate the Calvin-Benson cycle and measurements were carried out at 200 µmol photons m^{-2} s^{-1}. Parameters related to PSI and PSII photochemical responses were directly obtained from the Dual-PAM-100 software (Klughammer *et al.*, 2008; Schreiber and Klughammer, 2008; Baker, 2008).

Chloroplast isolation

Intact chloroplasts were isolated from WT and *pfld*5-8 leaf 1 at 25 dpg using Percoll gradient centrifugation (Napier and Barnes, 1995). Chloroplasts were counted after appropriate dilutions using a Neubauer chamber and an Olympus BH2 microscope, by image analysis with ImageJ. Their *Chl* contents were measured spectroscopically at 652 nm after extraction in 80% (v/v) acetone (Napier and Barnes, 1995).

ROS determination

A modified version of the FOX II assay (DeLong *et al.*, 2002) was used to quantify the presence of peroxides in cleared leaf extracts throughout leaf development. Two-hundred mg of leaf tissue were ground in liquid nitrogen and extracted with 300 µL of an 80:20 ethanol/water mixture, containing 0.01% (w/v) butylated hydroxytoluene (BHT). After centrifugation at 3,000 *g* for 10 min, 30 µL of the supernatant were combined with 30 µL of 10 mM Tris–phenyl phosphine (TPP, a peroxide reducing agent) or the same volume of methanol, and incubated for 30 min at 25°C. One-hundred µL of FOX reagent (100 µM xylenol orange, 4 mM BHT, 250 µM ferrous ammonium sulphate, 25 mM H_2SO_4 in 90% methanol) were then added to each sample, and the absorbance at 560 nm was recorded 10 min after reagent addition. The absorbance differences between equivalent samples with or without TPP indicate the levels of peroxides, which were calculated using an H_2O_2 standard curve.

Proteasome activity and inhibition assays

Ubiquitin-dependent proteasome activity was measured spectrofluorometrically using the 7-amino-4-methylcoumarin (AMC)-labeled fluorogenic substrate succinate (Suc)-LLVY-AMC (Roche Sigma-Aldrich, St. Louis, MO) in cleared extracts of leaf 1 at different dpg (Üstün *et al.*, 2016; Üstün and Börnke, 2017). Briefly, 100 mg of leaf tissue were frozen in liquid nitrogen and ground in 200 µL of extraction buffer (50 mM HEPES-KOH, pH 7.2, 2 mM ATP, 2 mM dithiothreitol, 250 mM sucrose). After centrifugation, the protein concentration of the supernatant, as determined by the Bradford (1976) procedure, was adjusted to 1 µg μL^{-1} with extraction buffer. Fifty µL of the protein solution were mixed with 220 µL of proteolysis buffer (100 mM HEPES-KOH, pH 7.8, 5 mM $MgCl_2$, 10 mM KCl, 2 mM ATP). The reaction was started after 5 min at 30°C by the addition of 0.2 mM Suc-LLVY-AMC. Released AMC was measured every 2 min

between 0 and 120 min using a Synergy HTX spectrofluorometer (Biotek, Winooski, VT) with excitation at 360 nm and emission at 460 nm.

For proteasome inhibition assay, seedlings were grown on 0.8% (w/v) agar containing half-strength Murashige and Skoog (1962) medium (0.5 × MS-agar) until 4 dpg. Subsequently, the aerial part was dipped in 1 mL of 0.01% (v/v) Tween-20 aqueous solution containing 50 µM MG132 (Roche Sigma-Aldrich) in dimethylsulfoxide (DMSO) or the equivalent proportion of DMSO (control) for 30 s and finally transferred back to 0.5 × MS-agar for 7 more days. Shoots were then excised and their fresh weight determined.

RNA isolation and quantitative reverse-transcription (qRT)-PCR analysis

Total RNA was isolated from 100 mg of tobacco leaf tissue using the TriPure reagent (Roche Sigma-Aldrich), according to the manufacturer's instructions, and reverse-transcribed with the MMLV enzyme (Invitrogen, Carlsbad, CA) and oligo$(dT)_{12\text{-}18}$. Real-time PCR reactions were carried out in a Mastercycler® ep*realplex*^{4} thermocycler (Eppendorf, Hamburg, Germany) using Platinum Taq DNA polymerase (Invitrogen) and SYBR Green I (Roche Sigma-Aldrich) to monitor the synthesis of double-stranded DNA. Relative transcript levels were determined for each sample and normalized against the levels of tobacco elongation factor 1α (EF1α) cDNA (Schmidt and Delaney, 2010). Primers (Table S1) were designed using the "Primer3Plus" software with an annealing temperature of 55°C and purchased from Invitrogen.

Ploidy analysis

Nuclei extraction and population measurements were carried out as described by Fina et al. (2017), with minor modifications. Briefly, ten leaves 1 from individual plants of each genotype at 25 dpg were cut in ~1-mm slices with a razor blade in 1 mL of a medium containing 30 mM sodium citrate, 20 mM 3-[N-morpholino] propane-sulfonic acid, pH 7.0, 45 mM $MgCl_2$, 1% (v/v) Triton X-100 (Galbraith *et al.*, 1991). Supernatants were then filtered through a 100 µm mesh, supplemented with 80 µL of 0.2 mg mL^{-1} propidium iodide, 50 mg mL^{-1} RNase, incubated for 30 min and read through a Cell Sorter BD FACSAria II flow cytometer (BD Biosciences, San Jose, CA). The endoreduplication index (EI) was calculated from the percentage values of each ploidy class with the

formula: EI = [(0 × %2C) +(1 × %4C) +(2 × %8C) + (3 × %16C) +(4 × %32C)]/100. Experiments were carried out in triplicate and at least 5,000 nuclei were analysed each time.

Statistical analyses

Data were analysed using one-way ANOVA and Tukey or Duncan multiple range tests. When the normality and/or equal variance assumptions were not met, Kruskall–Wallis one-way ANOVA between lines, and Dunn's multiple range tests were used. Significant differences refer to statistical significance at $P < 0.05$.

Acknowledgements

This research was funded by PICT-2015-3828 and PICT 2017-3080 from the National Agency for the Promotion of Science and Technology (ANPCyT, Argentina), and the Leibniz institute of Plant Genetics and Crop Plant Research (IPK). MM was a post-doctoral Fellow, and RA is a doctoral Fellow, both from the National Research Council (CONICET, Argentina). AL and NC are Staff Researchers from CONICET and Faculty members of the School of Biochemical and Pharmaceutical Sciences, University of Rosario (Facultad de Ciencias Bioquímicas y Farmacéuticas, Universidad Nacional de Rosario, Argentina). The authors wish to thank Diego Aguirre for his technical assistance with plant growth at IBR.

Conflict of Interest

The authors declare no conflict of interest.

Supporting information

Figure S1. Phenotypes of WT and Fld-expressing plants along development.

Figure S2. Expression of plastid-targeted Fld altered epidermal cell size but not cell number or stomatal index.

Figure S3. Fld expression in plastids did not alter cell size or number at the proliferative stage.

Figure S4. Chloroplast Fld decreased leaf 10 expansion compared to WT siblings.

Figure S5. Chloroplast-targeted Fld increased cell density in leaf 1 of *pfld* plants during leaf development.

Figure S6. Changes in photosynthetic pigments per area during development of WT and *pfld* leaves.

Figure S7. Changes in photosynthetic pigments per cell during development of WT and *pfld* leaves.

Figure S8. Fld expression in plastids did not affect chloroplast size or ultrastructure.

Table S1. Primers used for qRT-PCR determinations.

References

Andriankaja, M., Dhondt, S., de Bodt, S., et al. (2012) Exit from proliferation during leaf development in *Arabidopsis thaliana*: a not-so-gradual process. *Dev. Cell*, **22**, 64–78. doi: 10.1016/j.devcel.2011.11.011

Baker, N.R. (2008) Chlorophyll fluorescence: a probe of photosynthesis *in vivo*. *Annu. Rev. Plant Biol.*, **59**, 89–113. https://doi.org/10.1146/annurev.arplant.59.032607.092759

Bar, M. and Ori, N. (2014) Leaf development and morphogenesis. *Dev.*, **141**, 4219–4230. doi: 10.1242/dev.106195

Barkoulas, M., Hay, A., Kougioumoutzi, E. and Tsiantis, M. (2008) A developmental framework for dissected leaf formation in the Arabidopsis relative *Cardamine hirsuta*. *Nat. Genet.*, **40**, 1136–1141. doi: 10.1038/ng.189

Blanco, N.E., Ceccoli, R.D., Segretin, M.E., et al. (2011) Cyanobacterial flavodoxin complements ferredoxin deficiency in knocked-down transgenic tobacco plants. *Plant J.*, **65**, 922–935. doi: 10.1111/j.1365-

313X.2010.04479.x

Bradford, M.M. (1976) A rapid and sensitive method for the quantification of microgram quantities of protein utilising the principle of protein-dye binding. *Anal. Biochem*., **72**, 248–254. https://doi.org/10.1016/0003-2697(76)90527-3

Ceccoli, R.D., Blanco, N.E., Segretin, M.E., Melzer, M., Hanke, G.T., Scheibe, R., Hajirezaei, M.R., Bravo-Almonacid, F.F. and Carrillo, N. (2012) Flavodoxin displays dose-dependent effects on photosynthesis and stress tolerance when expressed in transgenic tobacco plants. *Planta*, **236**, 1447–1458. doi: 10.1007/s00425-012-1695-x

Cho, Y.H., Yoo, S.D. and Sheen, J. (2006) Regulatory functions of nuclear hexokinase1 complex in glucose signaling. *Cell*, **127**, 579–589. doi: 10.1016/j.cell.2006.09.028

Coba de la Peña, T., Redondo, F., Manrique, E., Lucas, M. and Pueyo, J. (2010) Nitrogen fixation persists under conditions of salt stress in transgenic *Medicago truncatula* plants expressing a cyanobacterial flavodoxin. *Plant Biotechnol. J.*, **8**, 954–965. doi: 10.1111/j.1467-7652.2010.00519.x.

Considine, M.J., Díaz-Vivancos, P., Kerchev, P., Signorelli, S., Agudelo-Romero, P., Gibbs, D.J. and Foyer, C.H. (2017) Learning to breathe: developmental phase transitions in oxygen status. *Trends Plant Sci.*, **22**, 140–153. doi: 10.1016/j.tplants.2016.11.013

DeLong, J.M., Prange, R.K., Hodges, D.M., Forney, C.F., Bishop, M.C. and Quilliam, M. (2002) Using a modified ferrous oxidation-xylenol orange (FOX) assay for detection of lipid hydroperoxides in plant tissue. *J. Agric. Food Chem.*, **50**, 248–254. doi: 10.1021/jf0106695.

Dietz, K.J., Turkan, I. and Krieger-Liszkay, A. (2016) Redox- and reactive oxygen species-dependent signaling into and out of the photosynthesizing chloroplast. *Plant Physiol.*, **171**, 1541–1550. doi: 10.1104/pp.16.00375

van Dingenen, J., Blomme, J., Gonzalez, N. and Inzé, D. (2016) Plants grow with a little help from their organelle friends. *J. Exp. Bot.*, **67**, 6267–6281.

doi:10.1093/jxb/erw399

van Dingenen, J., de Milde, L., Vermeersch, M., et al. (2016) Chloroplasts are central players in sugar-induced leaf growth. *Plant Physiol.*, **171**, 590-605. https://doi.org/10.1104/pp.15.01669

Disch, S., Anastasiou, E., Sharma, V.K., Laux, T., Fletcher, J.C. and Lenhard, M. (2006) The E3 ubiquitin ligase BIG BROTHER controls Arabidopsis organ size in a dosage-dependent manner. *Curr. Biol.*, **16**, 272–279. doi:10.1016/j.cub.2005.12.026

Donnelly, P.M., Bonetta, D., Tsukaya, H., Dengler, R.E. and Dengler, N.G. (1999) Cell cycling and cell enlargement in developing leaves of Arabidopsis. *Dev. Biol.*, **215**, 407–419. doi: 10.1006/dbio.1999.9443

Fina, J.P., Masotti, F., Rius, S.P., Crevacuore, F. and Casati, P. (2017) HAC1 and HAF1 histone acetyltransferases have different roles in UV-B responses in Arabidopsis. *Front. Plant Sci.*, **8**, 1179. https://doi.org/10.3389/fpls.2017.01179

Galbraith, D.W., Harkins, K.R. and Knapp, S. (1991) Systemic endopolyploidy in *Arabidopsis thaliana*. *Plant Physiol.*, **96**, 985–989. doi: 10.1104/pp.96.3.985

Gómez, R., Figueroa, N., Melzer, M., Hajirezaei, M.R., Carrillo, N. and Lodeyro, A.F. (2020) Photosynthetic characterization of flavodoxin-expressing tobacco plants reveals a high light acclimation-like phenotype. *Biochim. Biophys. Acta - Bioenerg.*, **1861**, 148211. doi: 10.1016/j.bbabio.2020.148211

Gómez, R., Vicino, P., Carrillo, N. and Lodeyro, A.F. (2019) Manipulation of oxidative stress responses as a strategy to generate stress-tolerant crops. From damage to signaling to tolerance. *Crit. Rev. Biotechnol.*, **39**, 693–708. https://doi.org/10.1080/07388551.2019.1597829

Gonzalez, N., de Bodt, S., Sulpice, R., et al. (2010) Increased leaf size: different means to an end. *Plant Physiol.*, **153**, 1261–1279. https://doi.org/10.1104/pp.110.156018

Gonzalez, N., Vanhaeren, H. and Inzé, D. (2012) Leaf size control: complex

coordination of cell division and expansion. *Trends Plant Sci.*, **17**, 332–340. doi: 10.1016/j.tplants.2012.02.003

Hernández-Verdeja, T. and Strand, Å. (2018) Retrograde signals navigate the path to chloroplast development. *Plant Physiol.*, **176**, 967–976. https://doi.org/10.1104/pp.17.01299

Huang, W., Suorsa, M. and Zhang, S.B. (2018) *In vivo* regulation of thylakoid proton motive force in immature leaves. *Photosynth. Res.*, **138**, 207–218. doi: 10.1007/s11120-018-0565-1

Hudik, E., Yoshioka, Y., Domenichini, S., et al. (2014) Chloroplast dysfunction causes multiple defects in cell cycle progression in the Arabidopsis crumpled leaf mutant. *Plant Physiol.*, **166**, 152–167. doi: 10.1104/pp.114.242628

Juvany, M., Müller, M. and Munné-Bosch, S. (2013) Photo-oxidative stress in emerging and senescing leaves: a mirror image? *J. Exp. Bot.*, **64**, 3087–3098. https://doi.org/10.1093/jxb/ert174

Kalve, S., de Vos, D. and Beemster, G.T.S. (2014) Leaf development: a cellular perspective. *Front. Plant Sci.*, **5**, 362. https://doi.org/10.3389/fpls.2014.00362

Kawade, K., Horiguchi, G., Ishikawa, N., Hirai, M.Y. and Tsukaya, H. (2013) Promotion of chloroplast proliferation upon enhanced post-mitotic cell expansion in leaves. *BMC Plant Biol.*, **13**, 143. https://doi.org/10.1186/1471-2229-13-143

Kazama, T., Ichihashi, Y., Murata, S. and Tsukaya, H. (2010) The mechanism of cell cycle arrest front progression explained by a KLUH/CYP78A5-dependent mobile growth factor in developing leaves of *Arabidopsis thaliana*. *Plant Cell Physiol.*, **51**, 1046–1054. doi: 10.1093/pcp/pcq051

Klughammer, C., Schreiber, U. and Walz, H. (2008) Complementary PS II quantum yields calculated from simple fluorescence parameters measured by PAM fluorometry and the Saturation Pulse method. *PAM Application Notes,* **1**, 27–35. https://www.walz.com/

Kraner, M.E., Link, K., Melzer, M., Ekici, A.B., Uebe, S., Tarazona, P.,

Feussner, I., Hofmann, J. and Sonnewald, U. (2017) Choline transporter-like1 (CHER1) is crucial for plasmodesmata maturation in *Arabidopsis thaliana*. *Plant J.*, **89**, 394–406. doi: 10.1111/tpj.13393

Kurepa, J. and Smalle, J.A. (2008) Structure, function and regulation of plant proteasomes. *Biochimie*, **90**, 324–335. doi: 10.1016/j.biochi.2007.07.019

Kurepa, J., Wang, S., Li, Y., Zaitlin, D., Pierce, A.J. and Smalle, J.A. (2009) Loss of 26S proteasome function leads to increased cell size and decreased cell number in Arabidopsis shoot organs. *Plant Physiol.*, **150**, 178–189. doi: 10.1104/pp.109.135970

Lefaki, M., Papaevgeniou, N. and Chondrogianni, N. (2017) Redox regulation of proteasome function. *Redox Biol.*, **13**, 452–458. https://doi.org/10.1016/j.redox.2017.07.005

Lepeduš, H., Gaća, V., Viljevac, M., Kovač, S., Fulgosi, H., Šimić, D., Jurković, V. and Cesar, V. (2011) Changes in photosynthetic performance and antioxidative strategies during maturation of Norway maple (*Acer platanoides* L.) leaves. *Plant Physiol. Biochem.*, **49**, 368–376. doi: 10.1016/j.plaphy.2010.12.011

Li, Z., Yuan, S., Jia, H., Gao, F., Zhou, M., Yuan, N., Wu, P., Hu, Q., Sun, D. and Luo, H. (2017) Ectopic expression of a cyanobacterial flavodoxin in creeping bentgrass impacts plant development and confers broad abiotic stress tolerance. *Plant Biotechnol. J.*, **15**, 433–446. doi: 10.1111/pbi.12638

Lichtenthaler, H.K. (1987) Chlorophylls and carotenoids: pigments of photosynthetic biomembranes. *Methods Enzymol.*, **148**, 350–382. https://doi.org/10.1016/0076-6879(87)48036-1

Lodeyro, A.F., Ceccoli, R.D., Pierella Karlusich, J.J. and Carrillo, N. (2012) The importance of flavodoxin for environmental stress tolerance in photosynthetic microorganisms and transgenic plants. Mechanism, evolution and biotechnological potential. *FEBS Lett.*, **586**, 2917–2924. doi: 10.1016/j.febslet.2012.07.026

Loudya, N., Okunola, T., He, J., Jarvis, P. and López-Juez, E. (2020) Retrograde signalling in a virescent mutant triggers an anterograde delay of

chloroplast biogenesis that requires GUN1 and is essential for survival. *Philos. Trans. R. Soc. B Biol. Sci.*, **375**. http://dx.doi.org/10.1098/rstb.2019.0400

Lu, D., Wang, T., Persson, S., Mueller-Roeber, B. and Schippers, J.H.M. (2014) Transcriptional control of ROS homeostasis by KUODA1 regulates cell expansion during leaf development. *Nat. Commun.*, **5**, 1–9. doi: 10.1038/ncomms4767

Mayta, M.L., Arce, R.C., Zurbriggen, M.D., Valle, E.M., Hajirezaei, M.R., Zanor, M.I. and Carrillo, N. (2019) Expression of a chloroplast-targeted cyanobacterial flavodoxin in tomato plants increases harvest index by altering plant size and productivity. *Front. Plant Sci.*, **10**, 1432. doi: 10.3389/fpls.2019.01432

Mayta, M.L., Lodeyro, A.F., Guiamet, J.J., Tognetti, V.B., Melzer, M., Hajirezaei, M.R. and Carrillo, N. (2018) Expression of a plastid-targeted flavodoxin decreases chloroplast reactive oxygen species accumulation and delays senescence in aging tobacco leaves. *Front. Plant Sci.*, **9**, 1039. doi: 10.3389/fpls.2018.01039

Muñoz, P. and Munné-Bosch, S. (2018) Photo-oxidative stress during leaf, flower and fruit development. *Plant Physiol.*, **176**, pp.01127.2017. doi: 10.1104/pp.17.01127

Murashige, T. and Skoog, F. (1962) A revised medium for rapid growth and bioassays with tobacco tissue culture. *Physiol. Plant.*, **15**, 473–497. https://doi.org/10.1111/j.1399-3054.1962.tb08052.x

Napier, J.A. and Barnes, S.A. (1995) The isolation of intact chloroplasts. *Methods Mol. Biol.*, **49**, 355–360. doi: 10.1385/0-89603-321-X:355.

Nelson, N. (2013) Evolution of photosystem I and the control of global enthalpy in an oxidizing world. *Photosynth. Res.*, **116**, 145–151. doi: 10.1007/s11120-013-9902-6

Nguyen, H.M., Schippers, J.H.M., Gõni-Ramos, O., Christoph, M.P., Dortay, H., van der Hoorn, R.A.L. and Mueller-Roeber, B. (2013) An upstream regulator of the 26S proteasome modulates organ size in *Arabidopsis*

thaliana. *Plant J.*, **74**, 25–36. doi: 10.1111/tpj.12097

Petrov, V., Hille, J., Mueller-Roeber, B. and Gechev, T.S. (2015) ROS-mediated abiotic stress-induced programmed cell death in plants. *Front. Plant Sci.*, **6**, 69. doi: 10.3389/fpls.2015.00069

Pfalz, J., Liebers, M., Hirth, M., Grübler, B., Holtzegel, U., Schröter, Y., Dietzel, L. and Pfannschmidt, T. (2012) Environmental control of plant nuclear gene expression by chloroplast redox signals. *Front. Plant Sci.*, **3**. https://doi.org/10.3389/fpls.2012.00257

Pierella Karlusich, J.J., Arce, R.C., Shahinnia, F., Sonnewald, S., Sonnewald, U., Zurbriggen, M.D., Hajirezaei, M.R. and Carrillo, N. (2020) Transcriptional and metabolic profiling of potato plants expressing a plastid-targeted electron shuttle reveal modulation of genes associated to drought tolerance by chloroplast redox poise. *Int. J. Mol. Sci.*, **21**, 1–22. doi: 10.3389/fpls.2019.01432

Pierella Karlusich, J.J., Ceccoli, R.D., Graña, M., Romero, H. and Carrillo, N. (2015) Environmental selection pressures related to iron utilization are involved in the loss of the flavodoxin gene from the plant genome. *Genome Biol. Evol.*, **7**, 750–767. doi: 10.1093/gbe/evv031

Pierella Karlusich, J.J., Lodeyro, A.F. and Carrillo, N. (2014) The long goodbye: the rise and fall of flavodoxin during plant evolution. *J. Exp. Bot.*, **65**, 5161–5178. doi: 10.1093/jxb/eru273

Pierella Karlusich, J.J., Zurbriggen, M.D., Shahinnia, F., Sonnewald, S., Sonnewald, U., Hosseini, S.A., Hajirezaei, M.R. and Carrillo, N. (2017) Chloroplast redox status modulates genome-wide plant responses during the non-host interaction of tobacco with the hemibiotrophic bacterium *Xanthomonas campestris* pv. *vesicatoria*. *Front. Plant Sci.*, **8**, 1158. https://doi.org/10.3389/fpls.2017.01158

Rasband, W.S. ImageJ, U. S. National Institutes of Health, Bethesda, Maryland, USA, https://imagej.nih.gov/ij/, 1997-2018.

Ren, T., Weraduwage, S.M. and Sharkey, T.D. (2019) Prospects for enhancing leaf photosynthetic capacity by manipulating mesophyll cell

morphology. *J. Exp. Bot.*, **70**, 1153–1165. doi: 10.1093/jxb/ery448

Rossi, F.R., Krapp, A.R., Bisaro, F., Maiale, S.J., Pieckenstain, F.L. and Carrillo, N. (2017) Reactive oxygen species generated in chloroplasts contribute to tobacco leaf infection by the necrotrophic fungus *Botrytis cinerea*. *Plant J.*, **92**, 761–773. doi: 10.1111/tpj.13718

Sako, K., Maki, Y., Imai, K.K., Aoyama, T., Goto, D.B. and Yamaguchi, J. (2010) Control of endoreduplication of trichome by RPT2a, a subunit of the 19S proteasome in Arabidopsis. *J. Plant Res.*, **123**, 701–706. https://doi.org/10.1007/s10265-010-0321-x

Sako, K. and Yamaguchi, J. (2010) How does the plant proteasome control leaf size? *Plant Signal. Behav.*, **5**, 1119–1120. doi: 10.4161/psb.5.9.12479

Schmidt, G.W. and Delaney, S.K. (2010) Stable internal reference genes for normalization of real-time RT-PCR in tobacco (*Nicotiana tabacum*) during development and abiotic stress. *Mol. Genet. Genomics*, **283**, 233–241. doi: 10.1007/s00438-010-0511-1

Schmidt, R., Kunkowska, A.B. and Schippers, J.H.M. (2016) Role of reactive oxygen species during cell expansion in leaves. *Plant Physiol.*, **172**, 2098–2106. https://doi.org/10.1104/pp.16.00426

Schreiber, U. and Klughammer, C. (2008) Non-photochemical fluorescence quenching and quantum yields in PS I and PS II: analysis of heat-induced limitations using Maxi-Imaging-PAM and Dual-PAM-100. *PAM Application Notes*, **1**, 15-18. http://www.walz.com/

Shimizu, T., Kacprzak, S.M., Mochizuki, N., et al. (2019) The retrograde signaling protein GUN1 regulates tetrapyrrole biosynthesis. *Proc. Natl. Acad. Sci. U. S. A.*, **116**, 24900–24906. https://doi.org/10.1073/pnas.1911251116

Smeekens, S. and Hellmann, H.A. (2014) Sugar sensing and signaling in plants. *Front. Plant Sci.*, **5**. doi: 10.3389/fpls.2014.00113

Sonoda, Y., Sako, K., Maki, Y., Yamazaki, N., Yamamoto, H., Ikeda, A. and Yamaguchi, J. (2009) Regulation of leaf organ size by the Arabidopsis RPT2a 19S proteasome subunit. *Plant J.*, **60**, 68–78. doi: 10.1111/j.1365-

313X.2009.03932.x

Su, J., Yang, L., Zhu, Q., Wu, H., He, Y., Liu, Y., Xu, J., Jiang, D. and Zhang, S. (2018) Active photosynthetic inhibition mediated by MPK3/MPK6 is critical to effector-triggered immunity. *PLOS Biol.*, **16**, e2004122. doi: 10.1371/journal.pbio.2004122

Szymańska, R. and Kruk, J. (2008) Tocopherol content and isomers' composition in selected plant species. *Plant Physiol. Biochem.*, **46**, 29–33. https://doi.org/10.1016/j.plaphy.2007.10.009

Tanaka, K. and Hanaoka, M. (2013) The early days of plastid retrograde signaling with respect to replication and transcription. *Front. Plant Sci.*, **3**. doi: 10.3389/fpls.2012.00301

Tognetti, V.B., Palatnik, J.F., Fillat, M.F., Melzer, M., Hajirezaei, M.R., Valle, E.M. and Carrillo, N. (2006) Functional replacement of ferredoxin by a cyanobacterial flavodoxin in tobacco confers broad-range stress tolerance. *Plant Cell*, **18**, 2035–2050. doi: 10.1105/tpc.106.042424

Tognetti, V.B., Zurbriggen, M.D., Morandi, E.N., Fillat, M.F., Valle, E.M., Hajirezaei, M.R. and Carrillo, N. (2007) Enhanced plant tolerance to iron starvation by functional substitution of chloroplast ferredoxin with a bacterial flavodoxin. *Proc. Natl. Acad. Sci.*, **104**, 11495–11500. doi: 10.1073/pnas.0704553104

Traas, J. and Monéger, F. (2010) Systems biology of organ initiation at the shoot apex. *Plant Physiol.*, **152**, 420–427. https://doi.org/10.1104/pp.109.150409

Tsukaya, H. (2008) Controlling size in multicellular organs: focus on the leaf. *PLoS Biol.*, **6**, e174. doi: 10.1371/journal.pbio.0060174

Tsukaya, H. (2019) Re-examination of the role of endoreduplication on cell-size control in leaves. *J. Plant Res.*, **132**, 571–580. doi: 10.1007/s10265-019-01125-7

Tsvetkov, P., Myers, N., Eliav, R., Adamovich, Y., Hagai, T., Adler, J., Navon, A. and Shaul, Y. (2014) NADH binds and stabilizes the 26S proteasomes independent of ATP. *J. Biol. Chem.*, **289**, 11272–11281. doi:

10.1074/jbc.M113.537175

Üstün, S. and Börnke, F. (2017) Ubiquitin proteasome activity measurement in total plant extracts. *Bio-protocol,* **7**, e2532. doi: 10.21769/BioProtoc.2532.

Üstün, S., Sheikh, A., Giménez-Ibáñez, S., Jones, A., Ntoukakis, V. and Börnke, F. (2016) The proteasome acts as a hub for plant immunity and is targeted by *Pseudomonas* type III effectors. *Plant Physiol.*, **172**, 1941–1958. doi: 10.1104/pp.16.00808

Vanhaeren, H., Nam, Y.-J., de Milde, L., Chae, E., Storme, V., Weigel, D., Gonzalez, N. and Inzé, D. (2017) Forever young: the role of ubiquitin receptor DA1 and E3 ligase BIG BROTHER in controlling leaf growth and development. *Plant Physiol*., **173**, 1269–1282. doi: 10.1104/pp.16.01410

Zurbriggen, M.D., Carrillo, N., Tognetti, V.B., Melzer, M., Peisker, M., Hause, B. and Hajirezaei, M.R. (2009) Chloroplast-generated reactive oxygen species play a major role in localized cell death during the non-host interaction between tobacco and *Xanthomonas campestris* pv. *vesicatoria*. *Plant J.*, **60**, 962–973. doi: 10.1111/j.1365-313X.2009.04010.x

Zurbriggen, M.D., Tognetti, V.B., Fillat, M.F., Hajirezaei, M.R., Valle, E.M. and Carrillo, N. (2008) Combating stress with flavodoxin: a promising route for crop improvement. *Trends Biotechnol.*, **26**, 531–537. doi:10.1016/j.tibtech.2008.07.001

Legends to Figures

Figure 1. Tobacco plants expressing a chloroplast-targeted Fld had smaller leaves. (a) Phenotypes of typical WT and Fld-expressing tobacco plants grown under chamber conditions at 35 dpg. Bar = 5 cm. (b) Phenotypes of leaf 1 from the same lines. Bar = 0.5 cm. (c) Areas of leaf 1 at 35 dpg determined by image analysis. (d) Leaf scheme showing where cell size and number were determined. Four regions of the leaf blade were used and their values averaged. (e) Representative micrographs from palisade parenchyma cells. The contour of typical cells is shown in red. Bar = 100 µm. (f, g) Cell areas (f) and cell numbers (g) were calculated from clarified leaf tissue, as indicated in

Experimental procedures. Data are presented as box plots of 11-14 biological replicates per genotype. Central lines show the medians; box limits indicate the 25th and 75th percentiles; whiskers extend 1.5 times the interquartile range from the 25th and 75th percentiles; grey filled circles or triangles represent data points. Asterisks indicate statistically significant differences ($P < 0.05$) determined using one-way ANOVA and Tukey multiple comparison test or Kruskall–Wallis one-way ANOVA and Dunn's multiple range test.

Figure 2. Leaves expressing a chloroplast-targeted Fld showed lower cell expansion rates. The first leaves of WT and *pfld* plants were collected at the indicated dpg for determination of leaf area and cell area and number. (a) Changes in leaf area during development. Data are means ± SD of at least 8 independent plants per line. (b) Average areas of adaxial sub-epidermal palisade parenchyma cells during leaf development. Cell areas were determined in 4 regions as indicated in Figure 1d. Data are represented as means ± SD (n = 100 cells from at least 8 leaves). (c) Changes in leaf cell number during development. Cells in the adaxial sub-epidermal palisade parenchyma layer were counted in individual leaves. Data are means ± SD from at least 8 leaves. Insets show a portion of the data that was magnified to show the absence of differences in the early stages of leaf development. Asterisks indicate statistically significant differences between WT and both *pfld* lines ($P < 0.05$) determined using one-way ANOVA and Tukey multiple comparison test or Kruskall–Wallis one-way ANOVA and Dunn's multiple range test.

Figure 3. Expression of a plastid-targeted Fld modified chloroplast number and pigment contents. (a) Total *Chl* contents in isolated chloroplasts of mature leaf 1 from WT and *pfld* plants at 25 dpg. Data are means ± SD of 7-8 independent plants per line. (b) Chloroplast number, estimated from *Chl* (a+b) per cell (Figure S7c) and total *Chl* per chloroplast. Data are means ± SD of 7-8 independent plants per line. (c) Chloroplast coverage, calculated as the ratio between chloroplast area (Figure S8b) and cell area (Figure 2b). Data reported are means ± SD of 47-52 biological replicates per genotype. Asterisks indicate statistically significant differences ($P < 0.05$) determined using one-way ANOVA and Duncan's multiple comparison test.

Figure 4. Fld expression in plastids prevented the age-dependent decline of electron transport rates and attenuated ROS production at all developmental stages. Measurements of quantum yields of (a) PSI and (b) PSII (Φ_{PSI} and Φ_{PSII}, respectively) were carried out in leaf 10 (*n* = 5-7) at the indicated dpg. (c) Contents of total peroxides (–OOH) were determined in cleared extracts of leaf 10 (*n* = 3). Data reported are means ± SD, and asterisks indicate statistically significant differences ($P < 0.05$) determined using one-way ANOVA and Duncan's multiple comparison test.

Figure 5. Plastid-targeted Fld affected proteasome activity. (a) Scheme of plant proteasome structure showing selected target genes with its reported location and function. Transcript levels of the (b) *RPN9 subunit of the 19S Regulatory Particle of the proteasome* (*RPN9*), (c) *Alpha 6 subunit of the 20S Core Protease of the proteasome* (*α6-SU*), (d) *Proteasome maturation protein 1* (*UMP1*), (e) *Regulatory Particle AAA-ATPase 2a* (*RPT2a*) and (f) *Regulatory Particle AAA-ATPase5a* (*RPT5a*) were determined in leaf 1 of WT and *pfld*5-8 plants by qRT-PCR. Values are means ± SD of fold-changes in log2 scale relative to the levels estimated in leaf 1 from WT plants at 6 dpg (*n* = 6). (g) Changes in proteasome activity in cleared extracts of leaf 1 during development (*n* = 3). RFU, relative fluorescence units. (h) Comparison of shoot growth, measured as fresh weight (FW), in the presence of the proteasome inhibitor MG132. Bar = 0.5 cm. (i) Shoot biomass accumulation after MG132 treatment (*n* = 6-8). Data reported are means ± SD, and asterisks indicate statistically significant differences ($P < 0.05$) determined using one-way ANOVA and Tukey multiple comparison test.

Figure 6. Plants expressing chloroplast Fld exhibited lower endoreduplication. (a) Flow cytometry profiles of nuclear DNA contents of leaf 1 at 25 dpg. (b) Percentage of nuclear DNA contents in the 2C and 4C classes. (c) Endoreduplication index (EI). Data are shown as means ± SD of 3 biological replicates, each consisting of leaves from 10 independent plants per line. Asterisks indicate statistically significant differences with respect to WT plants ($P < 0.05$) as determined using one-way ANOVA and Tukey multiple comparison test.

Figure 7. Proposed model for Fld action in leaf development. (a) Schematic representations of photosynthesis (green) and ROS production (orange) during leaf development. Dotted lines were drawn based on similar models reported by Juvany *et al.* (2013) and Muñoz and Munné-Bosch (2018). Experimental data for ROS levels (triangles) and Φ_{PSII} (circles) were taken from Figure 4 and overimposed for comparison. (b) Proposed model for the effect of Fld on leaf development. Fld activity as electron sink modifies chloroplast redox poise (Gómez *et al.*, 2020) and ROS production (Figure 4c), altering retrograde signalling output. A consequence of this modification is induction of proteasome expression (Pierella Karlusich *et al.*, 2017, 2020) and activity (Figure 5g). It is likely that the effects of increased proteasome activity on leaf size involve inhibition of DNA endoreduplication, as reported previously (Sako *et al.*, 2010).

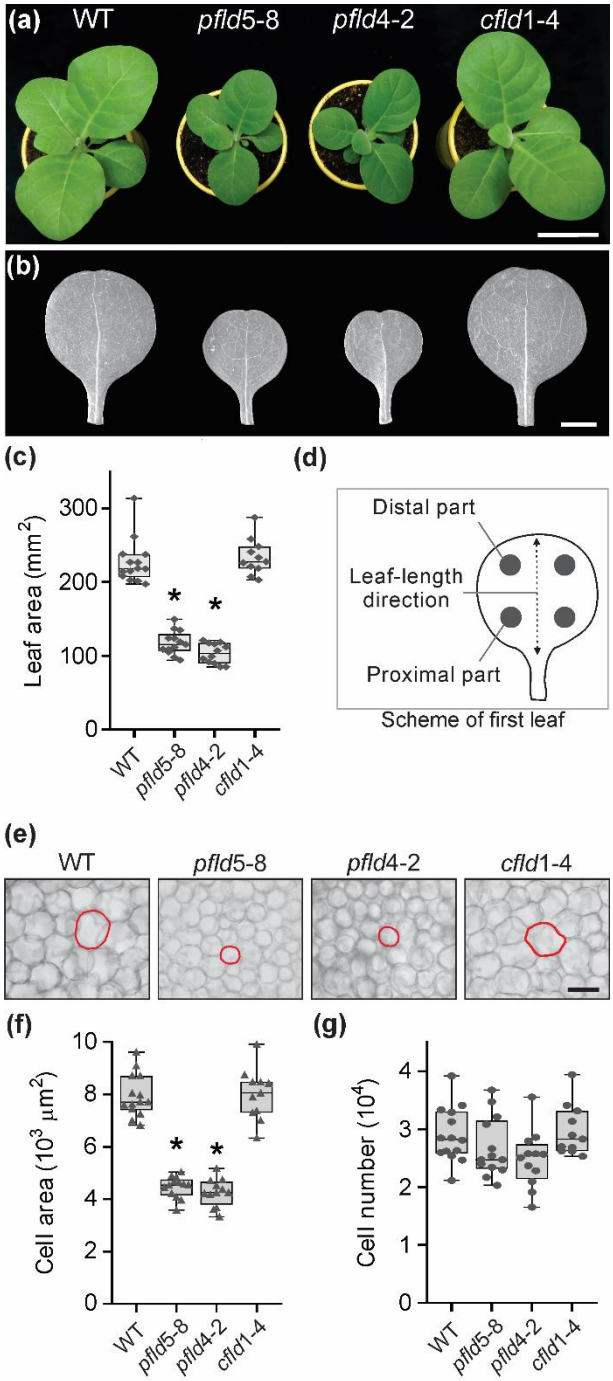
(a)
WT
pfld5-8
pfld4-2
cfld1-4
(b)
(c)
Leaf area (mm2)
300
200
100
0
*
*
WT
pfld5-8
pfld4-2
cfld1-4
(d)
Distal part
Leaf-length direction
Proximal part
Scheme of first leaf
(e)
WT
pfld5-8
pfld4-2
cfld1-4
(f)
Cell area (103 μm2)
10
8
6
4
2
0
*
*
WT
pfld5-8
pfld4-2
cfld1-4
(g)
Cell number (104)
4
3
2
1
0
WT
pfld5-8
pfld4-2
cfld1-4

Figure 1

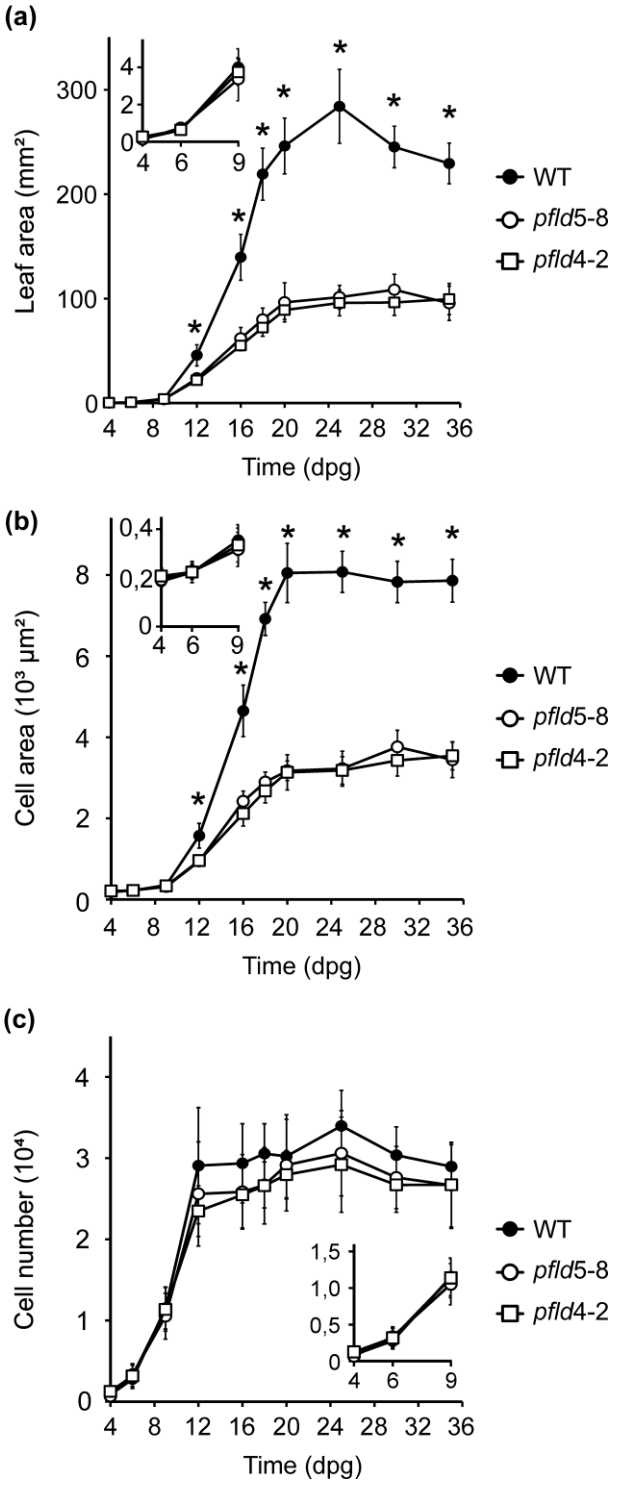
(a)
Leaf area (mm²)
Time (dpg)
WT
pfld5-8
pfld4-2
(b)
Cell area (10³ µm²)
Time (dpg)
WT
pfld5-8
pfld4-2
(c)
Cell number (10⁴)
Time (dpg)
WT
pfld5-8
pfld4-2

Figure 2

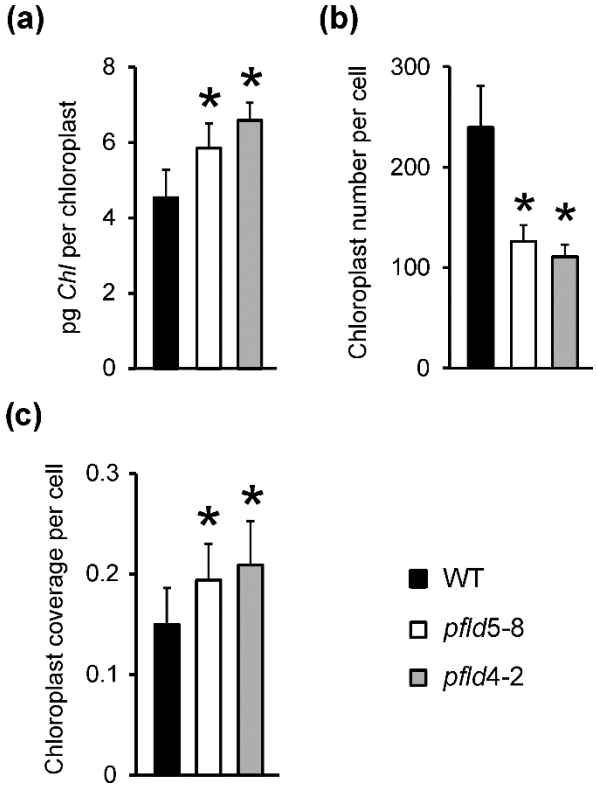
(a)
pg Chl per chloroplast
8
6
4
2
0
*
*
(b)
Chloroplast number per cell
300
200
100
0
*
*
(c)
Chloroplast coverage per cell
0.3
0.2
0.1
0
*
*
WT
pfld5-8
pfld4-2

Figure 3

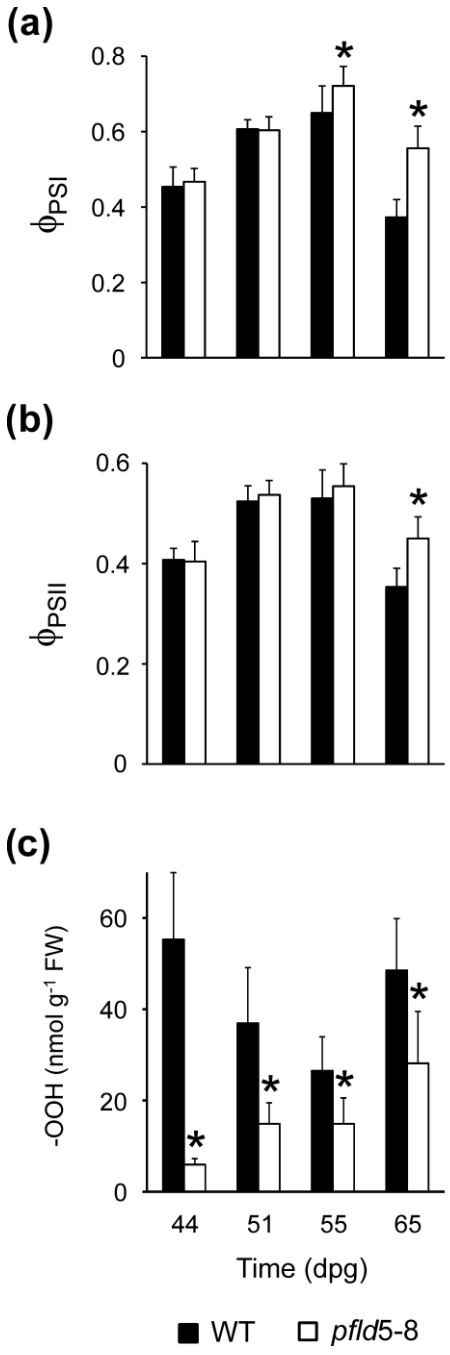
(a)
0.8
0.6
0.4
0.2
0
ϕPSI
*
*
(b)
0.6
0.4
0.2
0
ϕPSII
*
(c)
60
40
20
0
-OOH (nmol g-1 FW)
*
*
*
*
44
51
55
65
Time (dpg)
WT
pfld5-8

Figure 4

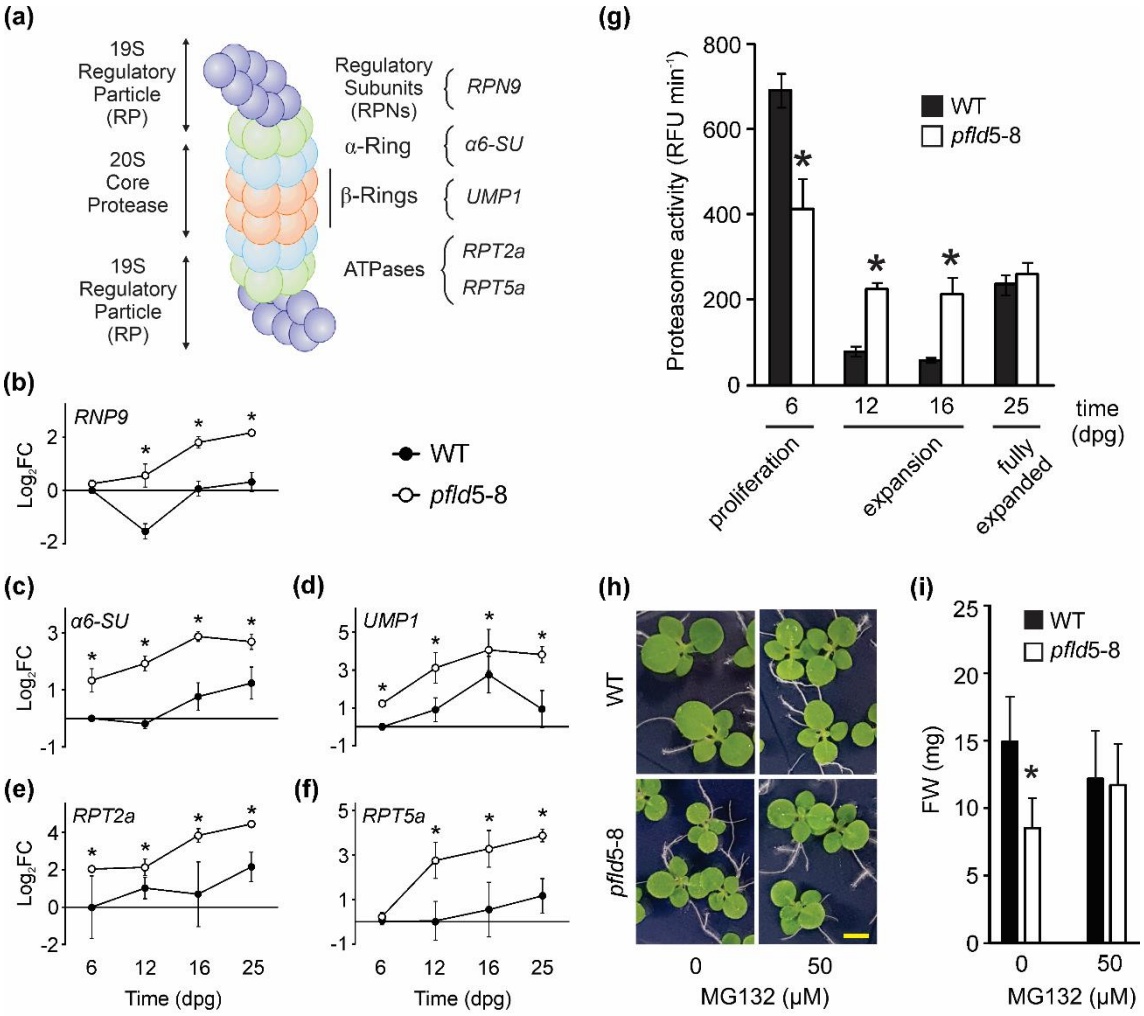
(a)
19S Regulatory Particle (RP)
20S Core Protease
19S Regulatory Particle (RP)
Regulatory Subunits (RPNs)
RPN9
α-Ring
α6-SU
β-Rings
UMP1
ATPases
RPT2a
RPT5a
(b)
RNP9
Log2FC
WT
pfld5-8
(c)
α6-SU
(d)
UMP1
(e)
RPT2a
(f)
RPT5a
Time (dpg)
(g)
Proteasome activity (RFU min-1)
WT
pfld5-8
time (dpg)
proliferation
expansion
fully expanded
(h)
WT
pfld5-8
MG132 (μM)
(i)
FW (mg)
WT
pfld5-8
MG132 (μM)

Figure 5

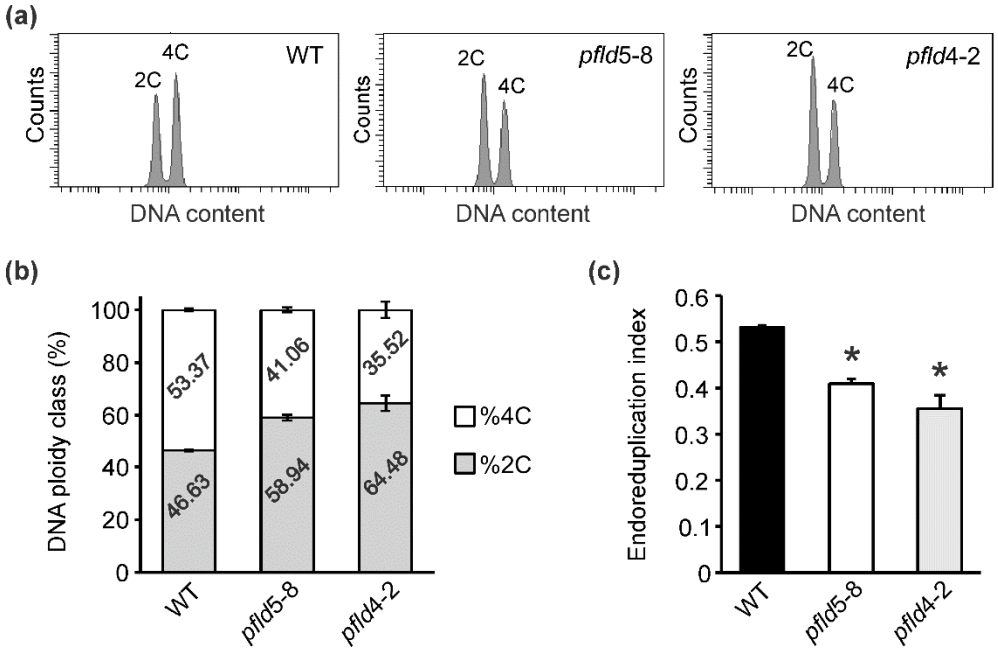
(a)
Counts
2C
4C
WT
DNA content
Counts
2C
4C
pfld5-8
DNA content
Counts
2C
4C
pfld4-2
DNA content
(b)
DNA ploidy class (%)
100
80
60
40
20
0
53.37
46.63
41.06
58.94
35.52
64.48
%4C
%2C
WT
pfld5-8
pfld4-2
(c)
Endoreduplication index
0.6
0.5
0.4
0.3
0.2
0.1
0
*
*
WT
pfld5-8
pfld4-2

Figure 6

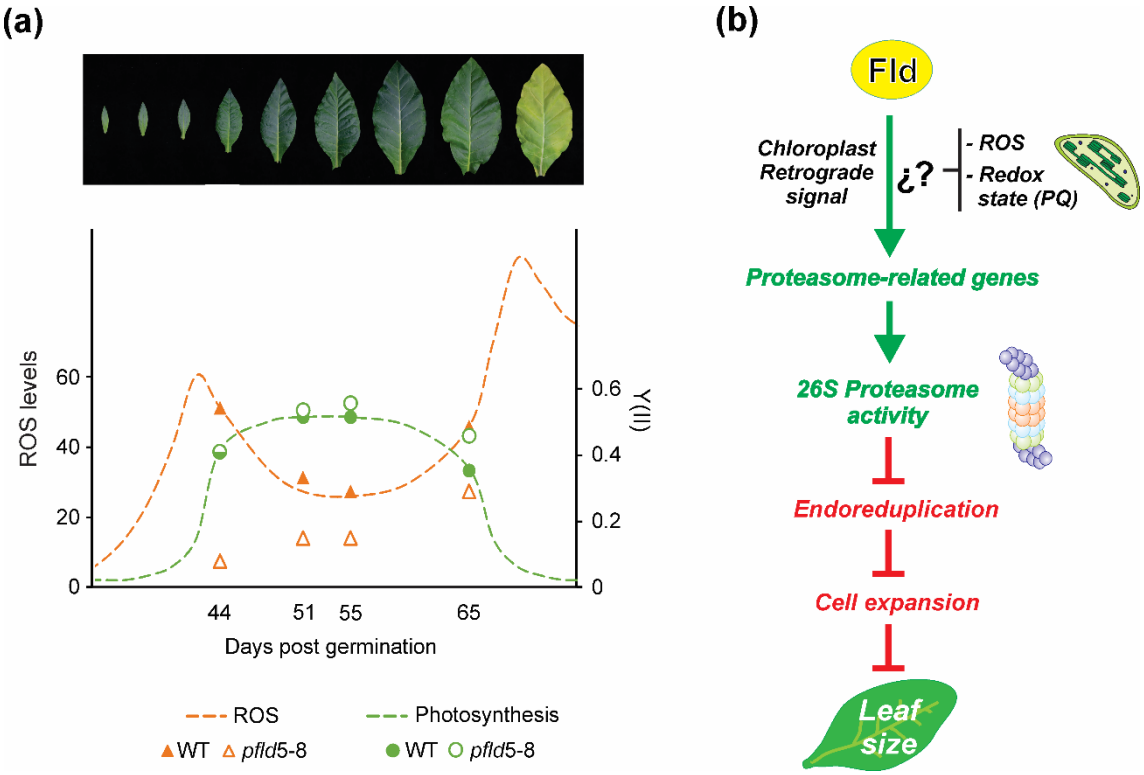
(a)
ROS levels
60
40
20
0
0.6
0.4
0.2
0
Y(II)
44
51
55
65
Days post germination
ROS
Photosynthesis
WT
pfld5-8
WT
pfld5-8
(b)
Fld
Chloroplast Retrograde signal
¿?
- ROS
- Redox state (PQ)
Proteasome-related genes
26S Proteasome activity
Endoreduplication
Cell expansion
Leaf size

Figure 7